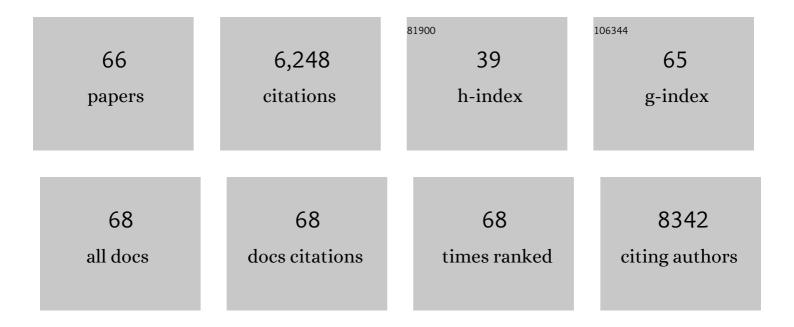
yelong Zhang

List of Publications by Year in descending order

Source: https://exaly.com/author-pdf/3711457/publications.pdf Version: 2024-02-01



#	Article	IF	CITATIONS
1	Cu ₁₂ Sb ₄ S ₁₃ Quantum Dots/Fewâ€Layered Ti ₃ C ₂ Nanosheets with Enhanced K ⁺ Diffusion Dynamics for Efficient Potassium Ion Storage. Advanced Functional Materials, 2022, 32, 2108574.	14.9	10
2	In-Situ growing tungsten Sulfide/Carbon nanosheets on sodium titanate nanorods to stabilize Surface-Structure for enhanced Sodium-ion storage. Journal of Colloid and Interface Science, 2022, 611, 609-616.	9.4	2
3	Cookies-like Ag2S/Bi4NbO8Cl heterostructures for high efficient and stable photocatalytic degradation of refractory antibiotics utilizing full-spectrum solar energy. Separation and Purification Technology, 2022, 292, 120969.	7.9	12
4	Dynamic Intercalation–Conversion Site Supported Ultrathin 2D Mesoporous SnO ₂ /SnSe ₂ Hybrid as Bifunctional Polysulfide Immobilizer and Lithium Regulator for Lithium–Sulfur Chemistry. ACS Nano, 2022, 16, 10783-10797.	14.6	63
5	Defective 1T′-ReSe2 nanosheets vertically grown on elastic MXene for fast and stable potassium ion storage. Science China Materials, 2022, 65, 3418-3427.	6.3	5
6	3D star-like atypical hybrid MOF derived single-atom catalyst boosts oxygen reduction catalysis. Journal of Energy Chemistry, 2021, 55, 355-360.	12.9	113
7	Progress and Perspective: MXene and MXeneâ€Based Nanomaterials for Highâ€Performance Energy Storage Devices. Advanced Electronic Materials, 2021, 7, 2000967.	5.1	122
8	Co _{0.7} Fe _{0.3} NPs confined in yolk–shell N-doped carbon: engineering multi-beaded fibers as an efficient bifunctional electrocatalyst for Zn–air batteries. Nanoscale, 2021, 13, 2609-2617.	5.6	19
9	SnS ₂ Nanosheets Anchored on Nitrogen and Sulfur Co-Doped MXene Sheets for High-Performance Potassium-Ion Batteries. ACS Applied Materials & Interfaces, 2021, 13, 17668-17676.	8.0	49
10	Orthorhombic Cobalt Ditelluride with Te Vacancy Defects Anchoring on Elastic MXene Enables Efficient Potassiumâ€lon Storage. Advanced Materials, 2021, 33, e2100272.	21.0	66
11	Strongly coupled Te-SnS2/MXene superstructure with self-autoadjustable function for fast and stable potassium ion storage. Journal of Energy Chemistry, 2021, 61, 416-424.	12.9	36
12	Defect-engineering of Pt/Bi ₄ NbO ₈ Br heterostructures for synergetic promotional photocatalytic removal of versatile organic contaminants. Journal of Materials Chemistry C, 2021, 9, 2784-2792.	5.5	13
13	Honeycomb-like 3D N-, P-codoped porous carbon anchored with ultrasmall Fe2P nanocrystals for efficient Zn-air battery. Carbon, 2020, 158, 885-892.	10.3	41
14	Stabilizing Niâ€Rich LiNi _{0.92} Co _{0.06} Al _{0.02} O ₂ Cathodes by Boracic Polyanion and Tungsten Cation Coâ€Doping for Highâ€Energy Lithiumâ€Ion Batteries. ChemElectroChem, 2020, 7, 3811-3817.	3.4	24
15	Metalâ€organic frameworkâ€derived Fe/Cuâ€substituted Co nanoparticles embedded in CNTsâ€grafted carbon polyhedron for Znâ€air batteries. , 2020, 2, 283-293.		95
16	In-situ construction of Bi/defective Bi4NbO8Cl for non-noble metal based Mott-Schottky photocatalysts towards organic pollutants removal. Journal of Hazardous Materials, 2020, 393, 122408.	12.4	54
17	A Freestanding Flexible Singleâ€Atom Cobaltâ€Based Multifunctional Interlayer toward Reversible and Durable Lithiumâ€6ulfur Batteries. Small Methods, 2020, 4, 1900701.	8.6	123
18	Synergistic effect between atomically dispersed Fe and Co metal sites for enhanced oxygen reduction reaction. Journal of Materials Chemistry A, 2020, 8, 4369-4375.	10.3	100

YELONG ZHANG

#	Article	IF	CITATIONS
19	A Highâ€Performance Carbonateâ€Free Lithium Garnet Interface Enabled by a Trace Amount of Sodium. Advanced Materials, 2020, 32, e2000575.	21.0	58
20	MXene-Ti ₃ C ₂ assisted one-step synthesis of carbon-supported TiO ₂ /Bi ₄ NbO ₈ Cl heterostructures for enhanced photocatalytic water decontamination. Nanophotonics, 2020, 9, 2077-2088.	6.0	31
21	Ni@RuM (M=Ni or Co) core@shell nanocrystals with high mass activity for overall water-splitting catalysis. Science China Materials, 2019, 62, 1868-1876.	6.3	21
22	Confined Fe ₂ VO ₄ âŠ,Nitrogenâ€Doped Carbon Nanowires with Internal Void Space for Highâ€Rate and Ultrastable Potassiumâ€lon Storage. Advanced Energy Materials, 2019, 9, 1902674.	19.5	81
23	Multidimensional Integrated Chalcogenides Nanoarchitecture Achieves Highly Stable and Ultrafast Potassiumâ€lon Storage. Small, 2019, 15, e1903720.	10.0	49
24	PdMo bimetallene for oxygen reduction catalysis. Nature, 2019, 574, 81-85.	27.8	935
25	MXene/Si@SiO _{<i>x</i>} @C Layer-by-Layer Superstructure with Autoadjustable Function for Superior Stable Lithium Storage. ACS Nano, 2019, 13, 2167-2175.	14.6	154
26	Ultrathin Ti3C2 nanosheets based "off-on―fluorescent nanoprobe for rapid and sensitive detection of HPV infection. Sensors and Actuators B: Chemical, 2019, 286, 222-229.	7.8	98
27	Bifunctional oxygen electrodes of homogeneous Co4N nanocrystals@N-doped carbon hybrids for rechargeable Zn-air batteries. Carbon, 2019, 151, 10-17.	10.3	67
28	Advanced Multifunctional Electrocatalysts for Energy Conversion. ACS Energy Letters, 2019, 4, 1672-1680.	17.4	78
29	Coupled and decoupled hierarchical carbon nanomaterials toward high-energy-density quasi-solid-state Na-Ion hybrid energy storage devices. Energy Storage Materials, 2019, 23, 530-538.	18.0	32
30	Strongly coupled ultrasmall-Fe ₇ C ₃ /N-doped porous carbon hybrids for highly efficient Zn–air batteries. Chemical Communications, 2019, 55, 5651-5654.	4.1	35
31	Polymerization-dissolution strategy to prepare Fe, N, S tri-doped carbon nanostructures for Zn-Air batteries. Carbon, 2019, 147, 83-89.	10.3	31
32	Efficient Bifunctional Polyalcohol Oxidation and Oxygen Reduction Electrocatalysts Enabled by Ultrathin PtPdM (M = Ni, Fe, Co) Nanosheets. Advanced Energy Materials, 2019, 9, 1800684.	19.5	112
33	Silk-Derived Highly Active Oxygen Electrocatalysts for Flexible and Rechargeable Zn–Air Batteries. Chemistry of Materials, 2019, 31, 1023-1029.	6.7	84
34	Strengthening reactive metal-support interaction to stabilize high-density Pt single atoms on electron-deficient g-C3N4 for boosting photocatalytic H2 production. Nano Energy, 2019, 56, 127-137.	16.0	247
35	Enhanced interaction in TiO ₂ /BiVO ₄ heterostructures via MXene Ti ₃ C ₂ -derived 2D-carbon for highly efficient visible-light photocatalysis. Nanotechnology, 2019, 30, 075601.	2.6	29
36	Ultrathin Visibleâ€Lightâ€Driven Mo Incorporating In ₂ O ₃ –ZnIn ₂ Se ₄ Zâ€6cheme Nanosheet Photocatalysts. Advanced Materials, 2019, 31, e1807226.	21.0	165

YELONG ZHANG

#	Article	IF	CITATIONS
37	Hollow Si/SiO _x nanosphere/nitrogen-doped carbon superstructure with a double shell and void for high-rate and long-life lithium-ion storage. Journal of Materials Chemistry A, 2018, 6, 8039-8046.	10.3	120
38	Rational Design of MXene/1Tâ€2H MoS ₂ Nanohybrids for Highâ€Performance Lithium–Sulfur Batteries. Advanced Functional Materials, 2018, 28, 1707578.	14.9	309
39	A Universal Strategy for Intimately Coupled Carbon Nanosheets/MoM Nanocrystals (M = P, S, C, and O) Hierarchical Hollow Nanospheres for Hydrogen Evolution Catalysis and Sodiumâ€lon Storage. Advanced Materials, 2018, 30, e1706085.	21.0	147
40	N-Doped Carbon Nanosheet Networks with Favorable Active Sites Triggered by Metal Nanoparticles as Bifunctional Oxygen Electrocatalysts. ACS Energy Letters, 2018, 3, 2914-2920.	17.4	107
41	Co ₃ O ₄ /Fe _{0.33} Co _{0.66} P Interface Nanowire for Enhancing Water Oxidation Catalysis at High Current Density. Advanced Materials, 2018, 30, e1803551.	21.0	150
42	Liquid-like Poly(ionic liquid) as Electrolyte for Thermally Stable Lithium-Ion Battery. ACS Omega, 2018, 3, 10564-10571.	3.5	18
43	One-Pot Seedless Aqueous Design of Metal Nanostructures for Energy Electrocatalytic Applications. Electrochemical Energy Reviews, 2018, 1, 531-547.	25.5	9
44	Metallic Grapheneâ€Like VSe ₂ Ultrathin Nanosheets: Superior Potassiumâ€lon Storage and Their Working Mechanism. Advanced Materials, 2018, 30, e1800036.	21.0	341
45	Rational Design of Hierarchical TiO ₂ /Epitaxially Aligned MoS ₂ –Carbon Coupled Interface Nanosheets Core/Shell Architecture for Ultrastable Sodiumâ€ion and Lithium–Sulfur Batteries. Small Methods, 2018, 2, 1800119.	8.6	49
46	Visible light-driven methanol dehydrogenation and conversion into 1,1-dimethoxymethane over a non-noble metal photocatalyst under acidic conditions. Catalysis Science and Technology, 2018, 8, 3372-3378.	4.1	35
47	Two-Dimensional Water-Coupled Metallic MoS ₂ with Nanochannels for Ultrafast Supercapacitors. Nano Letters, 2017, 17, 1825-1832.	9.1	337
48	Bioinspired Ultrastable Lignin Cathode via Graphene Reconfiguration for Energy Storage. ACS Sustainable Chemistry and Engineering, 2017, 5, 3553-3561.	6.7	51
49	Mesoporous nanostructured spinel-type MFe2O4 (M = Co, Mn, Ni) oxides as efficient bi-functional electrocatalysts towards oxygen reduction and oxygen evolution. Electrochimica Acta, 2017, 245, 829-838.	5.2	102
50	Porous ZrNb ₂₄ O ₆₂ nanowires with pseudocapacitive behavior achieve high-performance lithium-ion storage. Journal of Materials Chemistry A, 2017, 5, 22297-22304.	10.3	71
51	<i>In situ</i> formed Fe–N doped metal organic framework@carbon nanotubes/graphene hybrids for a rechargeable Zn–air battery. Chemical Communications, 2017, 53, 12934-12937.	4.1	76
52	Identifying Reactive Sites and Transport Limitations of Oxygen Reactions in Aprotic Lithiumâ€O ₂ Batteries at the Stage of Sudden Death. Angewandte Chemie, 2016, 128, 5287-5291.	2.0	20
53	Identifying Reactive Sites and Transport Limitations of Oxygen Reactions in Aprotic Lithiumâ€O ₂ Batteries at the Stage of Sudden Death. Angewandte Chemie - International Edition, 2016, 55, 5201-5205.	13.8	147
54	Amorphous Li ₂ O ₂ : Chemical Synthesis and Electrochemical Properties. Angewandte Chemie - International Edition, 2016, 55, 10717-10721.	13.8	135

YELONG ZHANG

#	Article	IF	CITATIONS
55	Metal–Organic Framework-Induced Synthesis of Ultrasmall Encased NiFe Nanoparticles Coupling with Graphene as an Efficient Oxygen Electrode for a Rechargeable Zn–Air Battery. ACS Catalysis, 2016, 6, 6335-6342.	11.2	210
56	Amorphous Li ₂ 0 ₂ : Chemical Synthesis and Electrochemical Properties. Angewandte Chemie, 2016, 128, 10875-10879.	2.0	37
57	Spectroscopic Identification of the Au–C Bond Formation upon Electroreduction of an Aryl Diazonium Salt on Gold. Langmuir, 2016, 32, 11514-11519.	3.5	14
58	Understanding oxygen reactions in aprotic Li-O ₂ batteries. Chinese Physics B, 2016, 25, 018204.	1.4	9
59	Dealloyed silver nanoparticles as efficient catalyst towards oxygen reduction in alkaline solution. Chemical Research in Chinese Universities, 2016, 32, 106-111.	2.6	5
60	Potential-Dependent Generation of O ₂ [–] and LiO ₂ and Their Critical Roles in O ₂ Reduction to Li ₂ O ₂ in Aprotic Li–O ₂ Batteries. Journal of Physical Chemistry C, 2016, 120, 3690-3698.	3.1	149
61	Polyphenylene Wrapped Sulfur/Multi-Walled Carbon Nano-Tubes via Spontaneous Grafting of Diazonium Salt for Improved Electrochemical Performance of Lithium-Sulfur Battery. Electrochimica Acta, 2015, 165, 136-141.	5.2	29
62	Li 2 O 2 oxidation: the charging reaction in the aprotic Li-O 2 batteries. Science Bulletin, 2015, 60, 1227-1234.	9.0	18
63	Reversibility of Noble Metal-Catalyzed Aprotic Li-O ₂ Batteries. Nano Letters, 2015, 15, 8084-8090.	9.1	165
64	Unlocking the energy capabilities of micron-sized LiFePO4. Nature Communications, 2015, 6, 7898.	12.8	65
65	Comparative study of two carbon fiber cathodes and theoretical analysis in microbial fuel cells on ocean floor. Journal of Ocean University of China, 2014, 13, 257-261.	1.2	4
66	Graphite coated with manganese oxide/multiwall carbon nanotubes composites as anodes in marine benthic microbial fuel cells. Applied Surface Science, 2014, 317, 84-89.	6.1	65